

## Type II seesaw models with modular $A_4$ symmetry

Tatsuo Kobayashi,<sup>1,\*</sup> Takaaki Nomura,<sup>2,†</sup> and Takashi Shimomura<sup>3,‡</sup>

<sup>1</sup>*Department of Physics, Hokkaido University, Sapporo 060-0810, Japan*

<sup>2</sup>*School of Physics, KIAS, Seoul 02455, Korea*

<sup>3</sup>*Faculty of Education, Miyazaki University, Miyazaki, 889-2192, Japan*

(Dated: December 3, 2019)

### Abstract

We discuss type-II seesaw models adopting modular  $A_4$  symmetry in supersymmetric framework. In our approach, the models are classified by the assignment of  $A_4$  representations and modular weights for leptons and triplet Higgs fields. Then neutrino mass matrix is characterized by modulus  $\tau$  and two free parameters. Carrying out numerical analysis, we find allowed parameter sets which can fit the neutrino oscillation data. For the allowed parameter sets, we obtain the predictions in neutrino sector such as CP violating phases and the lightest neutrino mass. Finally we also show the predictions for the branching ratios of doubly charged scalar boson focusing on the case where the doubly charged scalar boson dominantly decays into charged leptons.

---

\* kobayashi@particle.sci.hokudai.ac.jp

† nomura@kias.re.kr

‡ shimomura@cc.miyazaki-u.ac.jp

## I. INTRODUCTION

Understanding of the flavor structure of leptons and quarks is one of the well motivated issues to construct a model of new physics beyond the standard model (SM). In describing new physics, a new symmetry can play an important role to organize flavor structure.

The modular symmetry is a geometrical symmetry of torus and orbifold compactification, and very interesting, because it includes finite subgroups such as  $S_3$ ,  $A_4$ ,  $S_4$ , and  $A_5$  [1]. Zero-modes in superstring theory on such compactifications and its low-energy effective field theory transform non-trivially each other [2–7].<sup>1</sup> Inspired by these aspects, the framework of modular flavor symmetries have been recently proposed by [11] to realize more predictable structure in the quark and lepton sectors where a coupling can be transformed under a non-trivial representation of a non-Abelian discrete group. The typical groups in the framework are found in basis of the  $A_4$  modular group [11–25],  $S_3$  [26–29],  $S_4$  [30–36],  $A_5$  [35, 37, 38], multiple modular symmetries [39], and double covering of  $A_4$  [40] in which masses, mixing angles, and CP phases for quarks and leptons are predicted.<sup>2</sup> Possible corrections coming from Kähler potential are also considered in Ref. [49], and a systematic approach to understand the origin of CP transformations is discussed in Ref. [9, 50]. Also CP violation in models with modular symmetry is discussed in Ref. [51]. In applying a modular symmetry it is especially interesting to consider a new physics model generating neutrino masses since we would obtain the predictions for signals of new physics and observables in the neutrino sector, which can be correlated each other.

In realizing small neutrino masses, the so-called type-II seesaw mechanism is one of the interesting ideas in which an  $SU(2)$  triplet Higgs field is introduced [52–54]. The neutrino masses are generated through Yukawa interactions among the triplet and lepton doublets after the triplet developing a vacuum expectation value (VEV). In this scenario, we have a doubly charged scalar boson from the triplet which couples to charged leptons. The doubly charged scalar boson dominantly decays into the same sign charged lepton pair when the triplet VEV is less than around  $10^{-4}$  GeV, and it can give clear signals at the collider experiments such as the LHC. Importantly the branching ratios (BRs) of such decays are given by Yukawa couplings associated with neutrino mass generation and we can obtain

<sup>1</sup> See also Refs. [8–10].

<sup>2</sup> Several reviews are helpful to understand the non-Abelian group and its applications to flavor structure [41–48].

	Lepton		Higgs			
	$L$	$(e_R, \mu_R, \tau_R)$	$T_1$	$T_2$	$H_u$	$H_d$
$SU(2)_L$	<b>2</b>	1	<b>3</b>	<b>3</b>	<b>2</b>	<b>2</b>
$U(1)_Y$	$-\frac{1}{2}$	1	1	-1	$\frac{1}{2}$	$-\frac{1}{2}$
$A_4$	3	$1, 1'', 1'$	Model (1), (3): 1	(1), (3): 1	(1), (3): 1	1
			Model (2), (4): $1''$	(2), (4): $1'$	(2), (4): $1'$	
$k_I$	Model (1), (2): -1	-1	0	0	0	0
	Model (3), (4): -2	0[-2] for case A[B]				

TABLE I. Assignments under  $SU(2)_L \times U(1)_Y \times A_4$  for leptons and scalar fields.

some correlations among the BRs and neutrino parameters.

In this paper, we apply the modular  $A_4$  symmetry to the type-II seesaw mechanism in supersymmetric framework. Then some possible models are classified by the assignments of  $A_4$  representations and modular weights to the leptons and the Higgs triplet. We then scan free parameters in these models and search for the region in which the neutrino oscillation data can be fitted. For the allowed parameter sets, we show the predictions of observables in the neutrino sector. Finally we show our predictions for the branching ratios of the doubly charged scalar boson applying the allowed parameter sets.

The paper is organized as follows. In section 2, we introduce our models. In section 3, we perform parameter scan to fit neutrino oscillation data and provide some predictions in observables in the neutrino sector. Also, we show the branching ratios of the doubly charged scalar boson applying the parameter sets accommodating with the neutrino oscillation data. Section 4 is our conclusion and discussions. In Appendix, we summarize formulae to fix the coupling coefficients for the Yukawa interactions associated with charged lepton masses.

## II. MODELS

In this section we show type-II seesaw models with modular  $A_4$  symmetry in supersymmetric framework under which superfields of leptons are non-trivially transformed by the modular symmetry. In the type-II seesaw mechanism, we introduce two  $SU(2)$  triplet su-

perfields  $T_1$  and  $T_2$  which have hypercharge  $Y = 1$  and  $-1$  respectively; here we need two triplet superfields for gauge anomaly cancellation. We then obtain superpotential of the form

$$w_\nu = \mathbf{y}_T L T_1 L + \lambda_1 H_d T_1 H_d + \lambda_2 H_u T_2 H_u + M_T T_1 T_2, \quad (1)$$

where  $L$  is superfield for lepton doublet, and  $H_u$  and  $H_d$  are superfields for the Higgs doublets with hypercharge  $\frac{1}{2}$  and  $-\frac{1}{2}$  respectively. From the superpotential, we obtain the VEV of the neutral component of the  $T_1$  scalar, denoted by  $\langle T_1 \rangle = v_{T_1}$ , as follows

$$v_{T_1} = \lambda_2 \frac{v_u^2}{2M_T}, \quad (2)$$

where  $v_u$  is that of the  $H_u$  scalar. The VEV provides neutrino mass term [54]. The superpotential terms relevant to the charged lepton masses are written by

$$w_e = \mathbf{y}_e e_R H_d L + \mathbf{y}_\mu \mu_R H_d L + \mathbf{y}_\tau \tau_R H_d L, \quad (3)$$

where superfields  $\{e_R, \mu_R, \tau_R\}$  correspond to right-handed charged leptons. These superpotential terms are required to be invariant under  $A_4$  symmetry with vanishing modular weight where the couplings can be modular forms associated with non-trivial  $A_4$  representations and having non-zero modular weights. Then models are distinguished by the assignments of  $A_4$  representations and modular weights for the leptons and scalar fields. In Table. I, we summarize the assignment of  $A_4$  representations and modular weights to the fields in our models. With these representations and weights of the fields, those of the Yukawa couplings are fixed. Then, the structure of superpotential are determined. The other sectors are assumed to be equivalent to the supersymmetric type II seesaw model [54] and we do not discuss in this paper <sup>3</sup>.

The Yukawa coupling constants can have the modular weights under the modular symmetry. The modular form of  $A_4$  triplet with weight 2,  $\mathbf{Y}_3^{(2)}(\tau)$ , is given by

$$\mathbf{Y}_3^{(2)}(\tau) = \begin{pmatrix} Y_1(\tau) \\ Y_2(\tau) \\ Y_3(\tau) \end{pmatrix} = \begin{pmatrix} 1 + 12q + 36q^2 + 12q^3 + \dots \\ -6q^{1/3}(1 + 7q + 8q^2 + \dots) \\ -18q^{2/3}(1 + 2q + 5q^2 + \dots) \end{pmatrix}, \quad q = e^{2\pi i \tau}, \quad (4)$$

---

<sup>3</sup> For model (2) and (4), we assign  $1''$  representation to superfield associated with  $u_R$  to obtain  $Q_L H_u u_R$  term, and we need to introduce singlet scalar  $\varphi$  under  $1''$  with non-zero VEV to generate  $H_u H_d$  term.

where  $\tau$  is a complex number. More precisely, the above modular forms can be written in terms of Dedekind eta-function  $\eta(\tau)$  and its derivative:

$$\begin{aligned} Y_1(\tau) &= \frac{i}{2\pi} \left( \frac{\eta'(\tau/3)}{\eta(\tau/3)} + \frac{\eta'((\tau+1)/3)}{\eta((\tau+1)/3)} + \frac{\eta'((\tau+2)/3)}{\eta((\tau+2)/3)} - \frac{27\eta'(3\tau)}{\eta(3\tau)} \right), \\ Y_2(\tau) &= \frac{-i}{\pi} \left( \frac{\eta'(\tau/3)}{\eta(\tau/3)} + \omega^2 \frac{\eta'((\tau+1)/3)}{\eta((\tau+1)/3)} + \omega \frac{\eta'((\tau+2)/3)}{\eta((\tau+2)/3)} \right), \\ Y_3(\tau) &= \frac{-i}{\pi} \left( \frac{\eta'(\tau/3)}{\eta(\tau/3)} + \omega \frac{\eta'((\tau+1)/3)}{\eta((\tau+1)/3)} + \omega^2 \frac{\eta'((\tau+2)/3)}{\eta((\tau+2)/3)} \right), \end{aligned} \quad (5)$$

where  $w = e^{2\pi i/3}$ . Equation (4) is their  $q$ -expansions. The modular forms with higher weights can be constructed by products of  $\mathbf{Y}_3^{(2)}(\tau)$ . Singlet modular forms with weight 4,  $Y_1^{(4)}$  and  $Y_{1'}^{(4)}$  are given by

$$Y_1^{(4)} = Y_1^2 + 2Y_1Y_3, \quad (6)$$

$$Y_{1'}^{(4)} = Y_3^2 + 2Y_1Y_2, \quad (7)$$

where the modular form of  $1''$  representation with weight 4 does not exist due to the relation  $Y_2^2 + 2Y_1Y_3 = 0$ . Furthermore the triplet modular form with weight 4,  $\mathbf{Y}_3^{(4)}$ , is constructed as

$$\mathbf{Y}_3^{(4)} \equiv \begin{pmatrix} Y_{3,1}^{(4)} \\ Y_{3,2}^{(4)} \\ Y_{3,3}^{(4)} \end{pmatrix} = \begin{pmatrix} Y_1^2 - Y_2Y_3 \\ Y_3^2 - Y_1Y_2 \\ Y_2^2 - Y_1Y_3 \end{pmatrix}. \quad (8)$$

### A. Model (1)

In this model we can write the superpotential term relevant to the neutrino masses as

$$w_\nu = y \mathbf{Y}_3^{(2)} L T_1 L + \lambda_1 H_d T_1 H_d + \lambda_2 H_u T_2 H_u + M_T T_1 T_2, \quad (9)$$

and the superpotential term relevant to the charged lepton masses,

$$w_e = \alpha e_R H_d \left( L \mathbf{Y}_3^{(2)} \right) + \beta \mu_R H_d \left( L \mathbf{Y}_3^{(2)} \right) + \gamma \tau_R H_d \left( L \mathbf{Y}_3^{(2)} \right). \quad (10)$$

The mass matrix for the charged leptons is given by

$$L_{ME} = \bar{\ell}_R M_E \ell_L, \quad M_E = \tilde{\gamma} Y_3 \text{diag}[\hat{\alpha}, \hat{\beta}, 1] \begin{pmatrix} \hat{Y}_1 & \hat{Y}_2 & 1 \\ 1 & \hat{Y}_1 & \hat{Y}_2 \\ \hat{Y}_2 & 1 & \hat{Y}_1 \end{pmatrix}, \quad (11)$$

where  $\ell$  denotes three generations of charged leptons,  $\tilde{\gamma} \equiv v_d \gamma / \sqrt{2}$ ,  $\hat{\alpha} \equiv \alpha / \gamma$ ,  $\hat{\beta} = \beta / \gamma$  and  $\hat{Y}_{1,2} \equiv Y_{1,2} / Y_3$ . Here  $v_d$  is the VEV of  $H_d$ . As in the SM, we can diagonalize the mass matrix by transforming lepton fields,  $\ell_{L(R)} \rightarrow V_{L(R)}^e \ell_{L(R)}$ , providing  $\text{diag}(m_e, m_\mu, m_\tau) = (V_R^e)^\dagger M_e V_L^e$ . The parameters  $\hat{\alpha}$  and  $\hat{\beta}$  are determined to provide charged lepton mass eigenvalues as given in Appendix.

After the neutral component of  $T_1$  developing its VEV,  $v_{T_1}$ , we obtain Majorana neutrino mass terms such as

$$L_{M_\nu} = \frac{y v_{T_1}}{3\sqrt{2}} \bar{\nu}'_{L_i} \begin{pmatrix} 2Y_1 & -Y_3 & -Y_2 \\ -Y_3 & 2Y_2 & -Y_1 \\ -Y_2 & -Y_1 & 2Y_3 \end{pmatrix}_{ij} \nu'_{L_j}, \quad (12)$$

where  $\nu'_{L_{i=1,2,3}}$  denotes the neutral fermion component of  $L$ . Note that  $\nu'_{L_i}$ s are not identified with  $\nu_{e,\mu,\tau}$ , the partners of the charged leptons in weak interaction, since they are in the basis where charged lepton mass matrix is not diagonalized. Then we find the lepton flavor basis by

$$(\nu'_1, \nu'_2, \nu'_3)^T = V_L^e (\nu_e, \nu_\mu, \nu_\tau)^T. \quad (13)$$

Thus the neutrino mass matrix in the flavor basis is given by

$$m_\nu = \frac{\sqrt{2} y v_T}{3} (V_L^e)^T \begin{pmatrix} 2Y_1 & -Y_3 & -Y_2 \\ -Y_3 & 2Y_2 & -Y_1 \\ -Y_2 & -Y_1 & 2Y_3 \end{pmatrix} V_L^e. \quad (14)$$

Notice that the mixing matrix  $V_L^e$  is involved in the neutrino mass matrix.

## B. Model (2)

In this model, we take the  $A_4$  representations of  $T_1$ ,  $T_2$  and  $H_u$  as  $1''$ ,  $1'$  and  $1'$  while the other setting is the same as model (1). Then the superpotential term relevant to the neutrino masses is

$$w_\nu = y \mathbf{Y}_3^{(2)}(\tau) L T_1 L + \lambda_2 H_u T_2 H_u + M_T T_1 T_2. \quad (15)$$

Note that we do not have  $\lambda_1 H_d T_1 H_d$  term compared to Eq. (9) where the term is irrelevant in realizing the type-II seesaw mechanism and absence of the term does not affect our analysis. For charged lepton mass term, the superpotential is the same as Eq. (10).

The neutrino mass matrix in this case is

$$m_\nu = \frac{\sqrt{2}y v_{T_1}}{3} (V_L^e)^T \begin{pmatrix} 2Y_2 & -Y_1 & -Y_3 \\ -Y_1 & 2Y_3 & -Y_2 \\ -Y_3 & -Y_2 & 2Y_1 \end{pmatrix} V_L^e, \quad (16)$$

where the structure is different from model (1).

### C. Model (3)

In this model, we take the modular weight  $-2$  for leptons and assignment under the  $A_4$  representation is the same as model (1). Then the superpotential term relevant to the neutrino masses is

$$w_\nu = y_1 \mathbf{Y}_3^{(4)}(\tau) (LT_1 L)_3 + y_2 Y_1^{(4)}(\tau) (LT_1 L)_1 + y_3 Y_{1'}^{(4)}(\tau) (LT_1 L)_{1'} \quad (17)$$

$$+ \lambda_1 H_d T_1 H_d + \lambda_2 H_u T_2 H_u + M_T T_1 T_2. \quad (18)$$

In this case, we have additional terms with free parameters since  $A_4$  singlet modular forms are also available when couplings should have the modular weight 4.

For charged lepton mass term, we consider two cases depending on modular weight assignment for right-handed charged leptons. In cases A and B, the modular weights of  $\ell_R$  are assigned to 0 and  $-2$ , respectively. Then case A has the same superpotential as Eq. (10). On the other hand, for case B we obtain the corresponding superpotential as

$$w_e = \alpha e_R H_d \left( L \mathbf{Y}_3^{(4)} \right) + \beta \mu_R H_d \left( L \mathbf{Y}_3^{(4)} \right) + \gamma \tau_R H_d \left( L \mathbf{Y}_3^{(4)} \right). \quad (19)$$

In this case, the charged lepton mass matrix is

$$M_E = \gamma Y_{3,3}^{(4)} \text{diag}[\hat{\alpha}, \hat{\beta}, 1] \begin{pmatrix} \hat{Y}_{3,1}^{(4)} & \hat{Y}_{3,2}^{(4)} & 1 \\ 1 & \hat{Y}_{3,1}^{(4)} & \hat{Y}_{3,2}^{(4)} \\ \hat{Y}_{3,2}^{(4)} & 1 & \hat{Y}_{3,1}^{(4)} \end{pmatrix}, \quad (20)$$

where  $\hat{Y}_{3,1(2)}^{(4)} \equiv Y_{3,1(2)}^{(4)}/Y_{3,3}^{(4)}$ . We separately analyze cases A and B since the charged lepton mass matrix affects the neutrino mass matrix through  $V_L^e$  as we discussed above.

The neutrino mass matrix in this case is

$$m_\nu = \sqrt{2} y_1 v_T (V_L^e)^T \left[ \frac{1}{3} \begin{pmatrix} 2Y_{3,1}^{(4)} & -Y_{3,3}^{(4)} & -Y_{3,2}^{(4)} \\ -Y_{3,3}^{(4)} & 2Y_{3,2}^{(4)} & -Y_{3,1}^{(4)} \\ -Y_{3,2}^{(4)} & -Y_{3,1}^{(4)} & 2Y_{3,3}^{(4)} \end{pmatrix} + \hat{y}_2 Y_1^{(4)} \begin{pmatrix} 1 & 0 & 0 \\ 0 & 0 & 1 \\ 0 & 1 & 0 \end{pmatrix} + \hat{y}_3 Y_{1'}^{(4)} \begin{pmatrix} 0 & 0 & 1 \\ 0 & 1 & 0 \\ 1 & 0 & 0 \end{pmatrix} \right] V_L^e, \quad (21)$$

where  $\hat{y}_{2,3} \equiv y_{2,3}/y_1$ .

#### D. Model (4)

In this model, we chose  $A_4$  singlet  $1''$  for triplet  $T$  and the other assignments are the same as model (3). Then the superpotential term relevant to the neutrino masses is

$$w_\nu = y_1 \mathbf{Y}_3^{(4)}(\tau)(LT_1L)_3 + y_2 Y_1^{(4)}(\tau)(LT_1L)_1 + y_3 Y_{1'}^{(4)}(\tau)(LT_1L)_{1''} \quad (22)$$

$$+ \lambda_2 H_u T_2 H_u + M_T T_1 T_2, \quad (23)$$

and it is the same as model (3) except for the  $A_4$  structure. The superpotential term relevant to the charged lepton masses is the same as model (3), and we also analyze cases A and B separately.

The neutrino mass matrix in this case is

$$m_\nu = \sqrt{2} y_1 v_{T_1} (V_L^e)^T \left[ \frac{1}{3} \begin{pmatrix} 2Y_{3,2}^{(4)} & -Y_{3,1}^{(4)} & -Y_{3,3}^{(4)} \\ -Y_{3,1}^{(4)} & 2Y_{3,3}^{(4)} & -Y_{3,2}^{(4)} \\ -Y_{3,3}^{(4)} & -Y_{3,2}^{(4)} & 2Y_{3,1}^{(4)} \end{pmatrix} + \hat{y}_2 Y_1^{(4)} \begin{pmatrix} 0 & 1 & 0 \\ 1 & 0 & 0 \\ 0 & 0 & 1 \end{pmatrix} + \hat{y}_3 Y_{1'}^{(4)} \begin{pmatrix} 1 & 0 & 0 \\ 0 & 0 & 1 \\ 0 & 1 & 0 \end{pmatrix} \right] V_L^e, \quad (24)$$

where  $\hat{y}_{2,3} \equiv y_{2,3}/y_1$ .

### III. NUMERICAL ANALYSIS

In this section, we carry out numerical analysis. Firstly the free parameters in each model are scanned to search for regions which accommodate with neutrino oscillation data. Here we parameterize the PMNS matrix  $U_{PMNS}$ , diagonalizing the neutrino mass matrix  $m_\nu$ , in terms of three mixing angles  $\theta_{ij}$  ( $i, j = 1, 2, 3; i < j$ ), one CP violating Dirac phase  $\delta_{CP}$ , and two Majorana phases  $\{\alpha_{21}, \alpha_{32}\}$  as follows:

$$U_{PMNS} = \begin{pmatrix} c_{12}c_{13} & s_{12}c_{13} & s_{13}e^{-i\delta_{CP}} \\ -s_{12}c_{23} - c_{12}s_{23}s_{13}e^{i\delta_{CP}} & c_{12}c_{23} - s_{12}s_{23}s_{13}e^{i\delta_{CP}} & s_{23}c_{13} \\ s_{12}s_{23} - c_{12}c_{23}s_{13}e^{i\delta_{CP}} & -c_{12}s_{23} - s_{12}c_{23}s_{13}e^{i\delta_{CP}} & c_{23}c_{13} \end{pmatrix} \begin{pmatrix} 1 & 0 & 0 \\ 0 & e^{i\frac{\alpha_{21}}{2}} & 0 \\ 0 & 0 & e^{i\frac{\alpha_{31}}{2}} \end{pmatrix}, \quad (25)$$

where  $c_{ij}$  and  $s_{ij}$  denote  $\cos \theta_{ij}$  and  $\sin \theta_{ij}$  respectively. Then we estimate the branching ratios of the doubly charged scalar boson focusing on the decays into the same sign charged lepton pairs using the allowed parameters explaining neutrino data.



## A. Fitting neutrino oscillation data and relevant predictions

Here we scan the free parameters in the models and try to fit the neutrino oscillation data. In our analysis, we adopt experimentally allowed ranges for neutrino mixing and mass squared differences at  $3\sigma$  range taken from ref. [55] as follows:

$$\begin{aligned}
|\Delta m_{\text{atm}}^2| &= [2.431 - 2.622]([2.413 - 2.606]) \times 10^{-3} \text{ eV}^2 \quad \text{for NO(IO),} \\
\Delta m_{\text{sol}}^2 &= [6.79 - 8.01] \times 10^{-5} \text{ eV}^2 \quad \text{for both NO and IO,} \\
\sin^2 \theta_{13} &= [0.02044 - 0.02437] ([0.02067 - 0.02461]) \quad \text{for NO(IO),} \\
\sin^2 \theta_{23} &= [0.428 - 0.624] ([0.433 - 0.623]) \quad \text{for NO(IO),} \\
\sin^2 \theta_{12} &= [0.275 - 0.350] \quad \text{for both NO and IO,}
\end{aligned} \tag{26}$$

where NO(IO) stands for normal(inverted) ordering for neutrino masses. Then the free parameters are scanned in the following range:

$$\begin{aligned}
|\text{Re}[\tau]| &\in [0.1, 2.0], \quad \text{Im}[\tau] \in [0.6, 2.0], \\
\hat{y}_{2,3} &\in [-1.0, 1.0] \quad \text{for model (3) and (4).}
\end{aligned} \tag{27}$$

The values of  $\sqrt{2}y\nu_{T_1}/3$  and  $\sqrt{2}y_1\nu_{T_1}$  are fixed to provide allowed range of  $|\Delta m_{\text{atm}}^2|$  taking the value of  $|\Delta m_{\text{atm}}^2|$  as input parameter.

For parameters accommodating with neutrino data, we compute the Jarlskog invariant,  $\delta_{CP}$  given by PMNS matrix elements  $U_{\alpha i}$ :

$$J_{CP} = \text{Im}[U_{e1}U_{\mu 2}U_{e2}^*U_{\mu 1}^*] = s_{23}c_{23}s_{12}c_{12}s_{13}c_{13}^2 \sin \delta_{CP}. \tag{28}$$

The Majorana phases are also estimated via other invariants  $I_1$  and  $I_2$ :

$$I_1 = \text{Im}[U_{e1}^*U_{e2}] = c_{12}s_{12}c_{13}^2 \sin\left(\frac{\alpha_{21}}{2}\right), \quad I_2 = \text{Im}[U_{e1}^*U_{e3}] = c_{12}s_{13}c_{13} \sin\left(\frac{\alpha_{31}}{2} - \delta_{CP}\right). \tag{29}$$

We also calculate the effective mass for  $0\nu\beta\beta$  decay given by

$$m_{ee} = |m_1c_{12}^2c_{13}^2 + m_2s_{12}^2c_{13}^2e^{i\alpha_{21}} + m_3s_{13}^2e^{i(\alpha_{31}-2\delta_{CP})}|. \tag{30}$$

### 1. Model (1)

In this model, the modulus  $\tau$  is the only free parameter in the neutrino mass matrix except for overall factors associated with  $y\nu_T$ . For NO, it is found that we can fit the values

of  $|\Delta m_{\text{atm}}^2|$ ,  $|\Delta m_{\text{sol}}^2|$  and  $\sin^2 \theta_{12}$ . However, the predicted values for the other mixing angles are  $\sin^2 \theta_{23} \sim 0.8[0.5]$  and  $\sin^2 \theta_{13} \sim 0.45[0.11]$  with Eq. (36)[(37)] for charged lepton mass diagonalization, and they cannot be fully fitted to the observed data. For IO, we find that only  $|\Delta m_{\text{atm}}^2|$  and  $|\Delta m_{\text{sol}}^2|$  can be consistent with the observed data.

### 2. Model (2)

This model is similar to model (1) except for the neutrino mass structure. For NO, it is found that we can fit the values of  $|\Delta m_{\text{atm}}^2|$ ,  $|\Delta m_{\text{sol}}^2|$  and  $\sin^2 \theta_{12}$ . However, the predicted values for the other mixing angles are  $\sin^2 \theta_{23} \sim 0.2$  and  $\sin^2 \theta_{13} \sim 0.45$  for both Eq. (36) and (37) solutions, and they cannot be fully fitted to the observed data. For IO, we find that only  $|\Delta m_{\text{atm}}^2|$  and  $|\Delta m_{\text{sol}}^2|$  can be consistent with the observed data as in the model (1).

### 3. Model (3)

In this model we can fit the neutrino oscillation data due to the additional free parameters  $\hat{y}_{2,3}$  compared to model (1) and (2). For cases A and B, the results are summarized as follows. **Case A:** For NO, we find the parameter sets which can fit the neutrino oscillation data when we adopt Eq. (36) for  $\hat{\alpha}$  and  $\hat{\beta}$ . The preferred value of  $\tau$  is found to be  $\text{Re}[\tau] \sim \pm 1, \pm 2$  and  $\text{Im}[\tau] \sim 1.0 - 1.1$ . Then we find predictions on planes of  $\{\sin^2 \theta_{23}, \delta_{CP}\}$ ,  $\{\sin^2 \theta_{23}, J_{CP}\}$ ,  $\{\alpha_{21}, \alpha_{31}\}$  and  $\{m_1, m_{ee}\}$  shown in Fig. 1. We find two preferred region for  $\sin^2 \theta_{23}$  as  $\sim [0.46, 0.48]$  and  $\sim [0.54, 0.61]$ . In these regions the Dirac CP phase is differently predicted where we find  $|\delta_{CP}| \lesssim 50^\circ$  in the first region and  $|\delta_{CP}| \sim 60^\circ$  in the second region. We also find clear correlation between  $\alpha_{21}$  and  $\alpha_{32}$  in the first region while  $|\alpha_{21}| \sim 50^\circ$  and  $|\alpha_{31}| \sim 140^\circ$  are predicted in the second region. The lightest neutrino mass and  $m_{ee}$  are restricted to be  $m_1 \sim [0.011 - 0.017]$  eV and  $m_{ee} \sim [0.011 - 0.018]$  eV in this case. Furthermore we find the sum of neutrino masses to be  $\sum m_\nu \sim [0.07, 0.09]$  eV. It is also found that IO case is disfavored where we cannot fit three mixing angles simultaneously when we fit the mass differences.

**Case B:** For NO, we find the parameter sets which can fit the neutrino oscillation data adopting both Eq. (36) and (37) for  $\hat{\alpha}$  and  $\hat{\beta}$ . The preferred value of  $\tau$  is found to be  $\text{Re}[\tau] \sim \pm 1$  and  $\text{Im}[\tau] \sim 0.7 - 0.8[1.6 - 2.0]$  for Eq. (36)[(37)]. Then we show our predictions

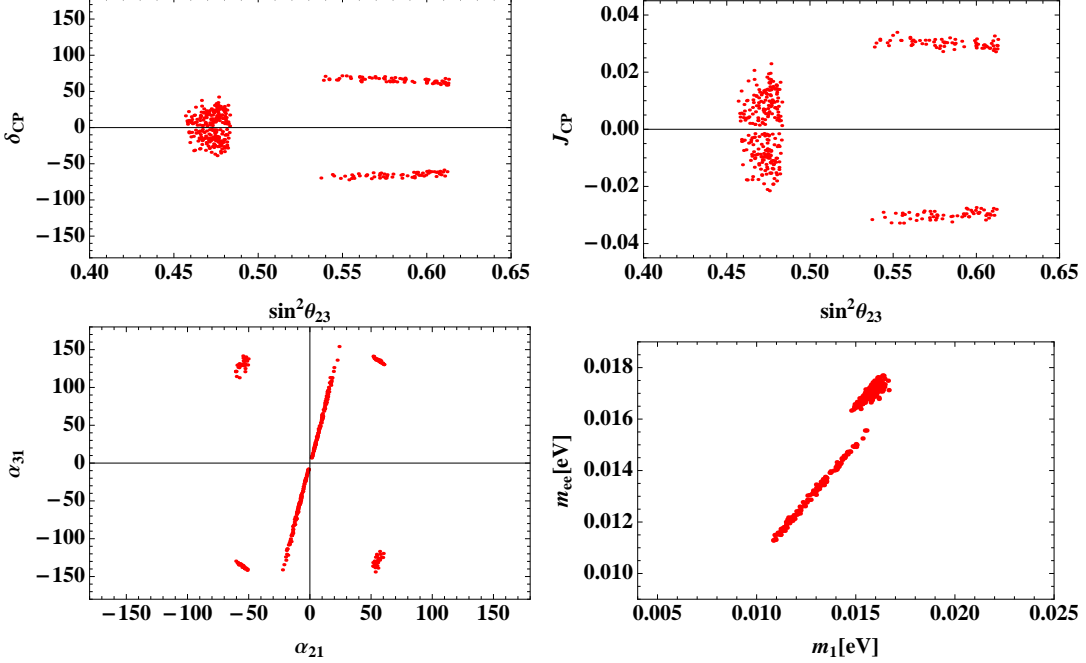


FIG. 1. Predictions in model (3) case A for NO. The upper-left panel: predicted values on  $\{\sin^2 \theta_{23}, \delta_{CP}\}$  plane. The upper-right panel: predicted values on  $\{\sin^2 \theta_{23}, J_{CP}\}$  plane. The lower-left panel: predicted values on  $\{\alpha_{21}, \alpha_{31}\}$  plane. The lower-right panel: predicted values on  $\{m_1, m_{ee}\}$  plane.

in Fig. 2 where red[blue] points correspond to the allowed parameter sets using Eq. (36)[(37)] for  $\hat{\alpha}$  and  $\hat{\beta}$ . The Dirac CP phase is found to be range of  $\pm 50^\circ$  to  $\pm 90^\circ$  in this case. We also find specific regions on  $\alpha_{21}$  and  $\alpha_{32}$  plane and the lightest neutrino mass is restricted to be  $m_1 \sim 0.02$  eV and  $\sim [0.03, 0.06]$  eV for Eq. (36) and (37) in this case. Furthermore we find  $m_{ee}$  and the sum of neutrino masses to be  $m_{ee} \sim [0.01, 0.02](0.02)$  eV and  $\sum m_\nu \sim [0.019, 0.022]([0.12, 0.19])$  eV for Eq. (36)( (37)). We also find the parameter sets which can fit the data for IO in this case when we adopt Eq. (37) for  $\hat{\alpha}$  and  $\hat{\beta}$ . The preferred value of  $\tau$  is found to be  $\text{Re}[\tau] \sim \pm 0.5$  to  $\sim 1$  and  $\text{Im}[\tau] \sim 1.7 - 1.8$ . Then we show our predictions in Fig. 3. The Dirac CP phase is found to be around  $\pm 50^\circ$  in this case. We also find specific regions on  $\alpha_{21}$  and  $\alpha_{32}$  plane and the lightest neutrino mass is restricted to be  $m_1 \sim [0.067 - 0.081]$  eV in this case. Furthermore we find  $m_{ee}$  and the sum of neutrino masses to be  $m_{ee} \sim [0.067, 0.081]$  eV and  $\sum m_\nu \sim [0.18, 0.22]$  eV. In this case the sum of neutrino masses is disfavored by the cosmological bound  $\sum m_\nu \lesssim 0.12$  eV [56].

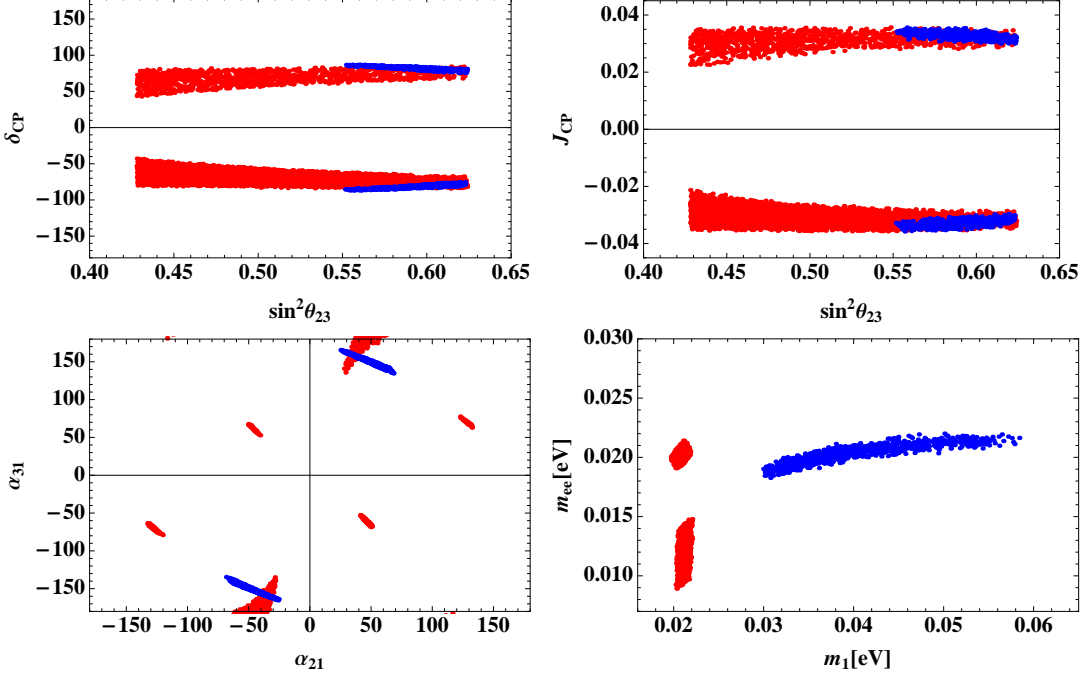


FIG. 2. The same plots as Fig. 1 in the case of Model (3) case B for NO where red[blue] points correspond to allowed parameter sets using Eq. (36)[(37)] for  $\hat{\alpha}$  and  $\hat{\beta}$ .

#### 4. Model (4)

This model can be also accommodated with the neutrino oscillation data due to the additional parameters. The results for cases A and B are as follows.

**Case A:** For NO, we find the parameter sets which can fit the neutrino oscillation data when we adopt Eq. (37) for  $\hat{\alpha}$  and  $\hat{\beta}$ . The preferred value of  $\tau$  is found to be  $\text{Re}[\tau] \sim 0, \pm 1, \pm 2$  and  $\text{Im}[\tau] \sim 0.8 - 1.1$ . Then we show our prediction on planes of  $\{\sin^2 \theta_{23}, \delta_{CP}\}$ ,  $\{\sin^2 \theta_{23}, J_{CP}\}$ ,  $\{\alpha_{21}, \alpha_{31}\}$  and  $\{m_1, m_{ee}\}$  in Fig. 4. We find specific regions on  $\alpha_{21}$  and  $\alpha_{32}$  plane. In addition, the lightest neutrino mass is restricted to be  $m_1 \sim [0.007 - 0.021]$  eV in this model. Furthermore we find  $m_{ee}$  and the sum of neutrino masses to be  $m_{ee} \sim [0.001, 0.020]$  eV and  $\sum m_\nu \sim [0.07, 0.10]$  eV. It is also found that IO case is disfavored where we cannot fit three mixing angles simultaneously when we fit the mass differences.

**Case B:** For NO, we find the parameter sets which can fit the neutrino oscillation data when we adopt Eq. (36) for  $\hat{\alpha}$  and  $\hat{\beta}$ . The preferred value of  $\tau$  is found to be  $\text{Re}[\tau] \sim \pm\{0.3, 0.6, 1.3, 1.6\}$  and  $\text{Im}[\tau] \sim 0.9 - 1.0$ . Then we show our predictions in Fig. 5. The Dirac CP phase is found to be around  $\pm 90^\circ$  in this case. We also find specific regions on

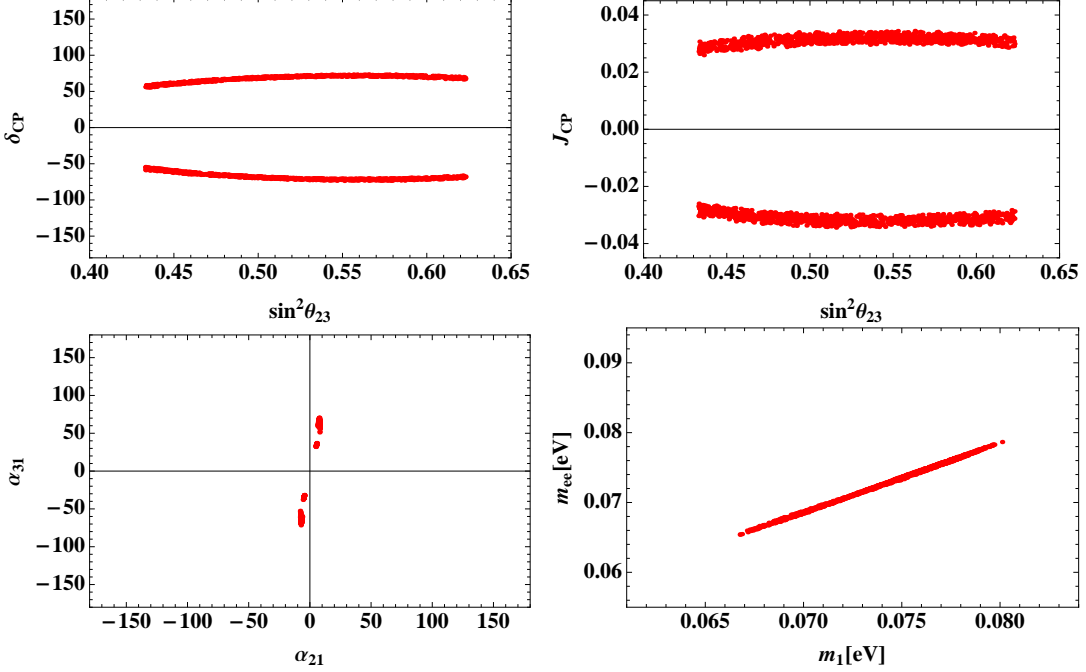


FIG. 3. The same plots as Fig. 1 in the case of Model (3) case B for IO.

$\alpha_{21}$  and  $\alpha_{32}$  plane and the lightest neutrino mass is restricted to be  $m_1 \sim [0.027 - 0.036]$  eV in this model which is slightly larger than the other results. Furthermore we find  $m_{ee}$  and the sum of neutrino masses to be  $m_{ee} \sim [0.027, 0.036]$  eV and  $\sum m_\nu \sim [0.11, 0.13]$  eV. It is also found that IO case is disfavored where we cannot fit three mixing angles simultaneously when we fit the mass differences.

## B. Branching ratio of doubly charged scalar boson

Here we calculate the branching ratios (BR) of the doubly charged scalar boson  $\delta^{\pm\pm}$ . In the type-II seesaw model,  $\delta^{\pm\pm} \rightarrow \ell^\pm \ell^\pm$  decay modes are induced via Yukawa couplings

$$L \supset \frac{1}{\sqrt{2}v_{T_1}} \bar{\ell}_{L_i}^c (m_\nu)_{ij} \ell_{L_j} \delta^{++} + h.c., \quad (31)$$

where  $m_\nu$  is the neutrino mass matrix. The doubly charged scalar also decays into same sign  $W$  boson pair through the gauge interaction which is proportional to  $v_{T_1}$ . Then leptonic modes are dominant when  $v_{T_1} < 10^{-4}$  GeV<sup>4</sup>. In our following analysis we focus on the

<sup>4</sup> We can also have decay modes with other scalar bosons in triplet. They can be ignored when masses for components of triplet are degenerated.

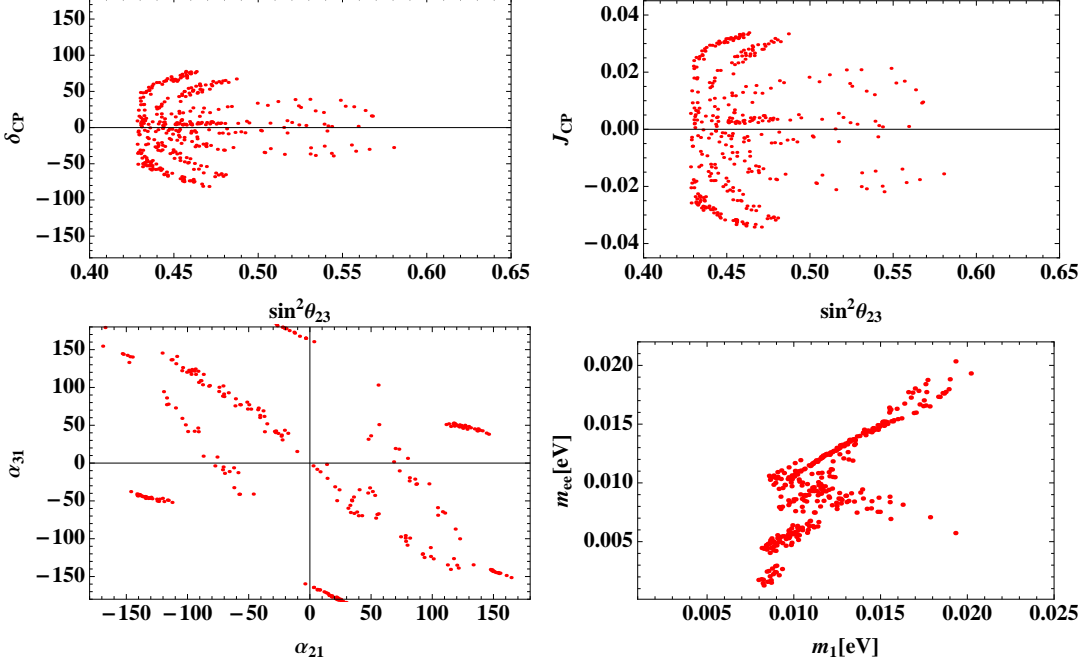


FIG. 4. The same plots as Fig. 1 in the case of Model (4) for NO.

case where leptonic modes are dominant choosing small  $v_{T_1}$  value since we are interested in prediction for leptonic decay BRs in the model. In addition, we assume the doubly charged scalar mass to be around TeV scale to avoid collider constraints [57–59]. In this case the BRs for leptonic modes are simply given by

$$BR(\delta^{\pm\pm} \rightarrow \ell_i^\pm \ell_j^\pm) \simeq \frac{1}{1 + \delta_{ij}} \frac{|(m_\nu)_{ij}|^2}{\sum_{k,l} |(m_\nu)_{kl}|^2 / (1 + \delta_{kl})}, \quad (32)$$

where we ignored decay width for  $\delta^{\pm\pm} \rightarrow W^\pm W^\pm$  and  $\delta_{ij}$  is the Kronecker delta. We then estimate the BRs for the parameter sets which can accommodate with the neutrino oscillation data in models (3) and (4).

### 1. Model (3)

In Fig. 6, we show predicted BRs for NO case applying the allowed parameter sets which accommodate with the neutrino oscillation data. In this model, we find two regions for the predicted BRs. One region indicates BRs for modes  $\{e^\pm \mu^\pm, \mu^\pm \mu^\pm, \tau^\pm \tau^\pm, e^\pm \mu^\pm, e^\pm \tau^\pm, \mu^\pm \tau^\pm\}$  as around  $\{0.1, 0.33, 0.37, 0.02, 0.01, 0.17\}$ , and this region corresponds to  $\sin^2 \theta_{23} \sim [0.46, 0.48]$ . The other region indicates BRs for  $\{e^\pm \mu^\pm, \mu^\pm \mu^\pm, \tau^\pm \tau^\pm, e^\pm \mu^\pm, e^\pm \tau^\pm, \mu^\pm \tau^\pm\}$  as around  $\{0.03-$

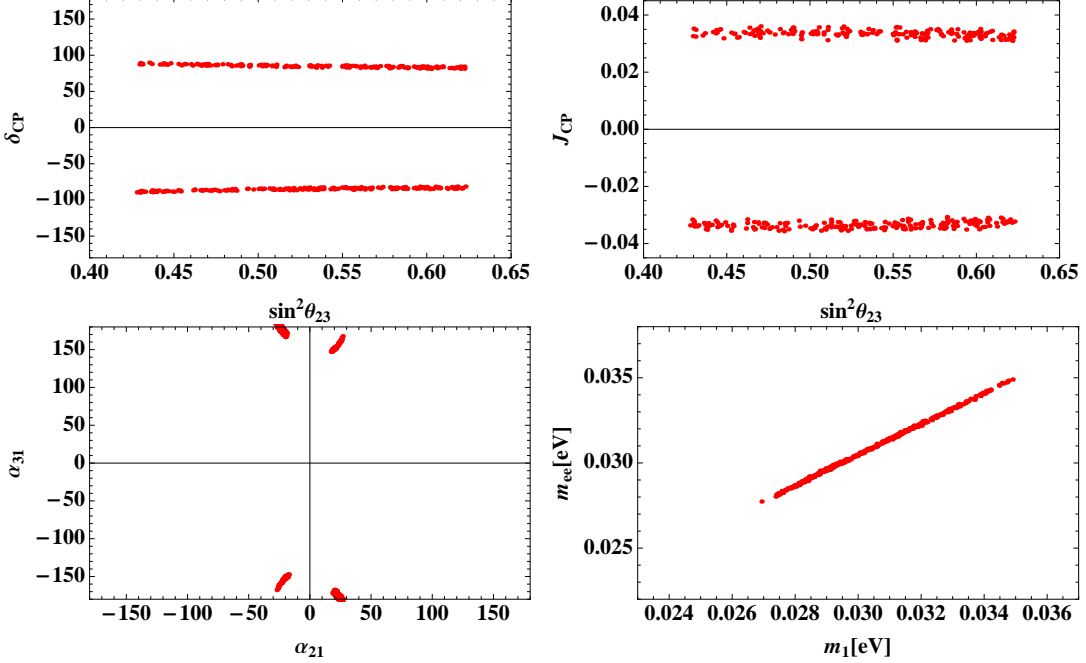


FIG. 5. The same plots as Fig. 1 in the case of Model (4) case B for NO.

$0.05, 0.35 - 0.4, 0.25 - 0.33, 0.05 - 0.1, 0 - 0.01, 0.2 - 0.25\}$ , and this region corresponds to  $\sin^2 \theta_{23} \sim [0.54, 0.61]$ . We predict that BR for the modes including electron tend to be small, and  $\mu^\pm \mu^\pm$  and  $\tau^\pm \tau^\pm$  modes have the largest value around  $0.33 - 0.37$ .

In Fig. 7, we show predicted BRs in case B for NO applying the allowed parameter sets. In this case, we also find two separate regions for predicted BRs corresponding to two solutions for  $\hat{\alpha}$  and  $\hat{\beta}$  where colors correspond to those in Fig. 2. Red region indicates BRs for  $\{e^\pm \mu^\pm, \mu^\pm \mu^\pm, \tau^\pm \tau^\pm, e^\pm \mu^\pm, e^\pm \tau^\pm, \mu^\pm \tau^\pm\}$  as around  $\{0.02 - 0.05, 0.1 - 0.22, 0.02 - 0.15, 0.01 - 0.05, 0.15, 0.55\}$ . In this region  $\mu^\pm \tau^\pm$  mode has the largest BR and the  $\mu^\pm \mu^\pm$  and  $e^\pm \tau^\pm$  modes also have sizable BRs.. The other region indicates BRs for  $\{e^\pm \mu^\pm, \mu^\pm \mu^\pm, \tau^\pm \tau^\pm, e^\pm \mu^\pm, e^\pm \tau^\pm, \mu^\pm \tau^\pm\}$  as around  $\{0.15 - 0.25, 0.01 - 0.1, 0 - 0.04, 0.01 - 0.05, 0.01 - 0.04, 0.62 - 0.64\}$ . In this region  $\mu^\pm \tau^\pm$  mode is also dominant and  $e^\pm e^\pm$  has sizable BR.

In Fig. 8, we show predicted BRs in case B for IO applying the allowed parameter sets. In this case, we find one region for predicted BRs. The plots indicate BRs for  $\{e^\pm \mu^\pm, \mu^\pm \mu^\pm, \tau^\pm \tau^\pm, e^\pm \mu^\pm, e^\pm \tau^\pm, \mu^\pm \tau^\pm\}$  as around  $\{0.37, 0.02 - 0.05, 0.01 - 0.08, \sim 0.02, \sim 0.02, 0.49 - 0.55\}$ . In this region  $\mu^\pm \tau^\pm$  and  $e^\pm e^\pm$  modes have dominant BR and the other modes are suppressed.

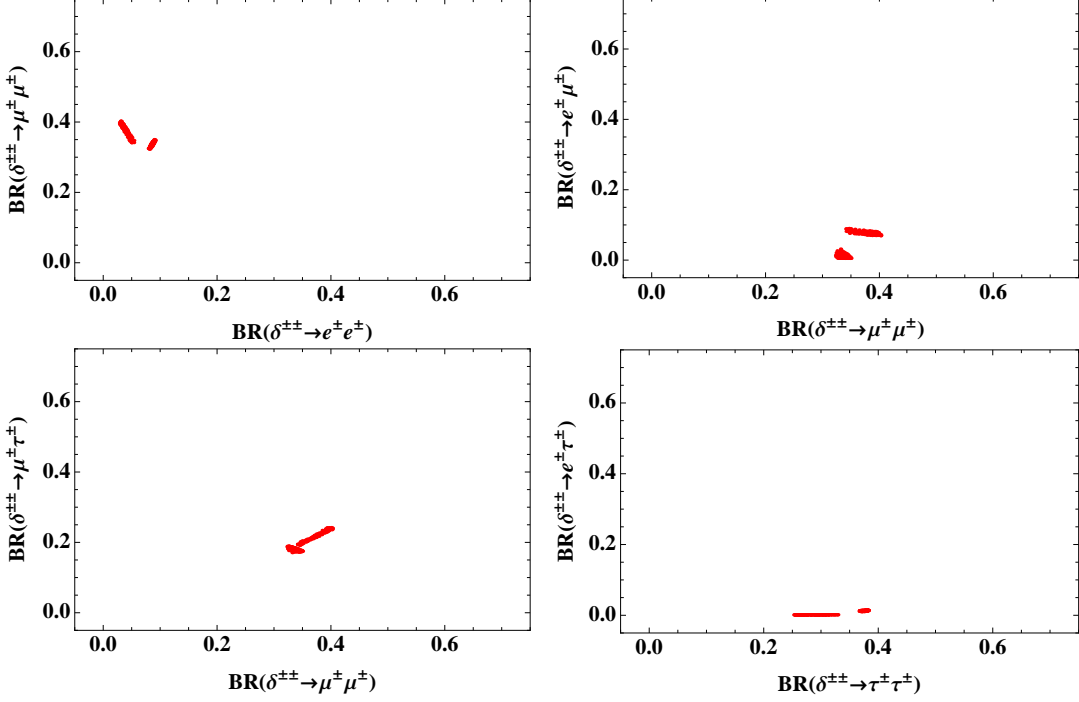


FIG. 6. Predictions of doubly charged scalar BRs in model (3) case A for NO. The upper-left panel: predicted BRs for  $\{e^\pm e^\pm, \mu^\pm \mu^\pm\}$  modes. The upper-right panel: predicted BRs for  $\{\mu^\pm \mu^\pm, e^\pm \mu^\pm\}$  modes. The lower-left panel: predicted BRs for  $\{\mu^\pm \mu^\pm, \mu^\pm \tau^\pm\}$  modes. The lower-right panel: predicted BRs for  $\{\tau^\pm \tau^\pm, e^\pm \tau^\pm\}$  modes.

## 2. Model (4)

In Fig. 9, we show predicted BRs in case A for NO applying the allowed parameter sets which accommodate with the neutrino oscillation data. In this case, we also find two separate regions for predicted BRs. One region indicates BRs for  $\{e^\pm \mu^\pm, \mu^\pm \mu^\pm, \tau^\pm \tau^\pm, e^\pm \mu^\pm, e^\pm \tau^\pm, \mu^\pm \tau^\pm\}$  as around  $\{0.02 - 0.07, 0.05 - 0.1, 0.15 - 0.2, 0.01 - 0.05, 0.01 - 0.05, 0.6 - 0.7\}$ . In this region  $\mu^\pm \tau^\pm$  mode has the largest BR and the other lepton flavor violating modes are suppressed. The other region indicates BRs for  $\{e^\pm \mu^\pm, \mu^\pm \mu^\pm, \tau^\pm \tau^\pm, e^\pm \mu^\pm, e^\pm \tau^\pm, \mu^\pm \tau^\pm\}$  as around  $\{0.01 - 0.05, 0.28 - 0.35, 0.15 - 0.38, 0 - 0.02, 0.04 - 0.2, 0.25\}$ . In this region  $e^\pm \mu^\pm$  mode is suppressed and the other modes have BRs of  $0.1 - 0.4$ .

In Fig. 10, we show predicted BRs in case B for NO applying allowed parameter sets which accommodate with neutrino data. In this case, we also find one region for predicted BRs. The plots indicate BRs for  $\{e^\pm \mu^\pm, \mu^\pm \mu^\pm, \tau^\pm \tau^\pm, e^\pm \mu^\pm, e^\pm \tau^\pm, \mu^\pm \tau^\pm\}$  as around  $\{0.15 -$



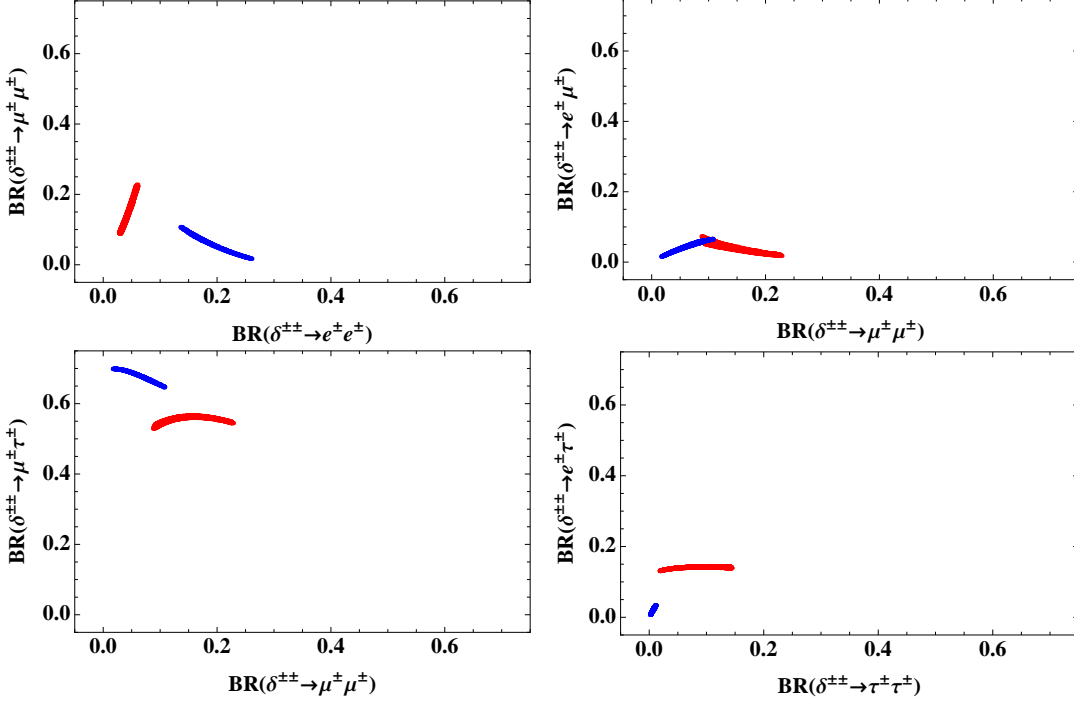


FIG. 7. The same plots as Fig. 6 in the case of Model (3) case B for NO.

$0.20, 0.0 - 0.1, 0.0 - 0.08, \sim 0, \sim 0, \sim 0.7\}$ . In this region  $\mu^\pm \tau^\pm$  mode has the largest BR and the other lepton flavor violating modes are suppressed. In addition,  $e^\pm e^\pm$  mode has the highest BR for flavor diagonal mode.

#### IV. CONCLUSION

We have discussed type-II seesaw models with modular  $A_4$  symmetry in supersymmetric framework. In our approach, models are classified by the assignment of  $A_4$  representations and modular weights for leptons and triplet Higgs field. The free parameters in models are scanned to fit the neutrino oscillation data and we find the minimal case including only weight 2 modular form is disfavored. We can fit the data for the models with weight 4 modular form applied to the neutrino mass matrix due to additional two free parameters. Then we have shown the predictions in the neutrino parameters for the allowed parameter sets accommodating with the neutrino oscillation data. Finally the branching ratios of the doubly charged scalar boson are calculated applying the allowed parameter sets focusing on the case where the doubly charged scalar dominantly decays into charged leptons choosing

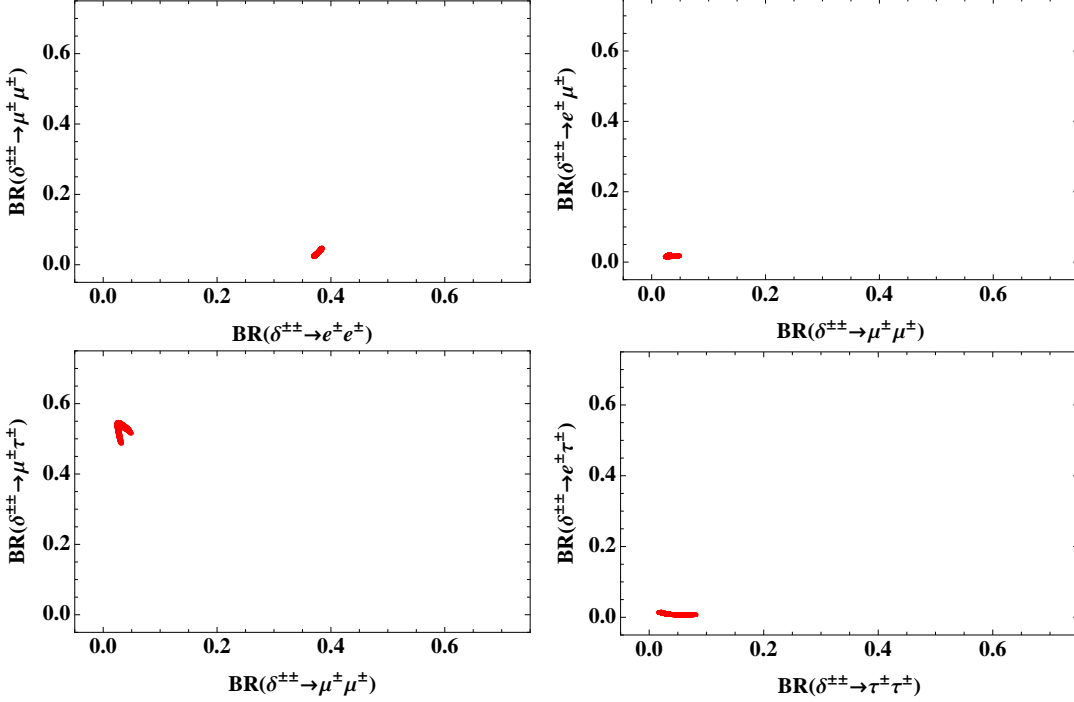


FIG. 8. The same plots as Fig. 6 in the case of Model (3) case B for IO.

small triplet VEV. We can predict the branching ratios where these values are realized to be in some restricted regions. Therefore it can be clear indication of our models if we find the pattern of the branching ratios at the collider experiment. Furthermore we have the relations between predictions in the neutrino parameters and the branching ratios. Importantly measurement of these branching ratios can test a flavor structure by modular symmetry comparing predictions in the neutrino sector.

Before closing the conclusion, we would like to comment on the other lepton flavor violating (LFV) processes such as  $\mu \rightarrow e\gamma$ ,  $\tau \rightarrow \mu(e)\gamma$  and  $\mu \rightarrow 3e$ , etc. As shown in the branching ratios of the doubly charged scalar boson, the elements of the neutrino mass matrix are constrained and related with each other due to modular  $A_4$  symmetry. Therefore it is expected that the BRs of the LFV processes will also have correlations among them. If it is the case, such correlations will provide another useful information which enable us to discriminate our model from others. The LFV BRs depend on the mass of the charged scalar bosons and need detailed analyses including the spectrum of the scalar bosons. Such analyses are beyond the scope of this paper and we will leave this for our future work.

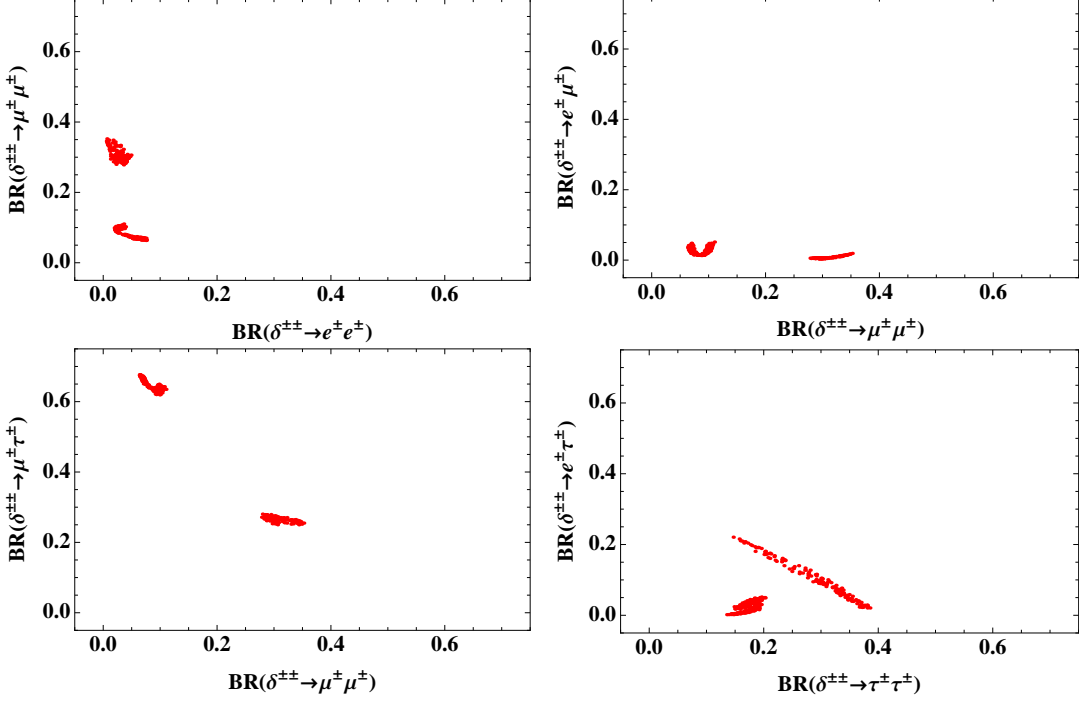


FIG. 9. The same plots as Fig. 6 in the case of Model (4) case A for NO.

## APPENDIX: DETERMINING FREE PARAMETERS IN CHARGED LEPTON MASS MATRIX

In this appendix we summarize determination of free parameters,  $\{\alpha, \beta, \gamma\}$ , in charged lepton mass matrix in Eq. (11) following discussion in ref. [13]. We have three equations with charged lepton mass eigenvalues:

$$\text{Tr}[M_E^\dagger M_E] = \sum_{i=e}^{\tau} m_i^2 = \frac{|\tilde{\gamma} Y_3|^2}{4} (1 + \hat{\alpha}^2 + \hat{\beta}^2), \quad (33a)$$

$$\text{Det}[M_E^\dagger M_E] = \prod_{i=e}^{\tau} m_i^2 = \frac{|\tilde{\gamma} Y_3|^6}{64} \hat{\alpha}^2 \hat{\beta}^2 C_2, \quad (33b)$$

$$\frac{\text{Tr}[M_E^\dagger M_E]^2 - \text{Det}[M_E^\dagger M_E]}{2} = \chi = \frac{|\tilde{\gamma} Y_3|^4}{16} (\hat{\alpha}^2 + \hat{\alpha}^2 \hat{\beta}^2 + \hat{\beta}^2) C_3, \quad (33c)$$

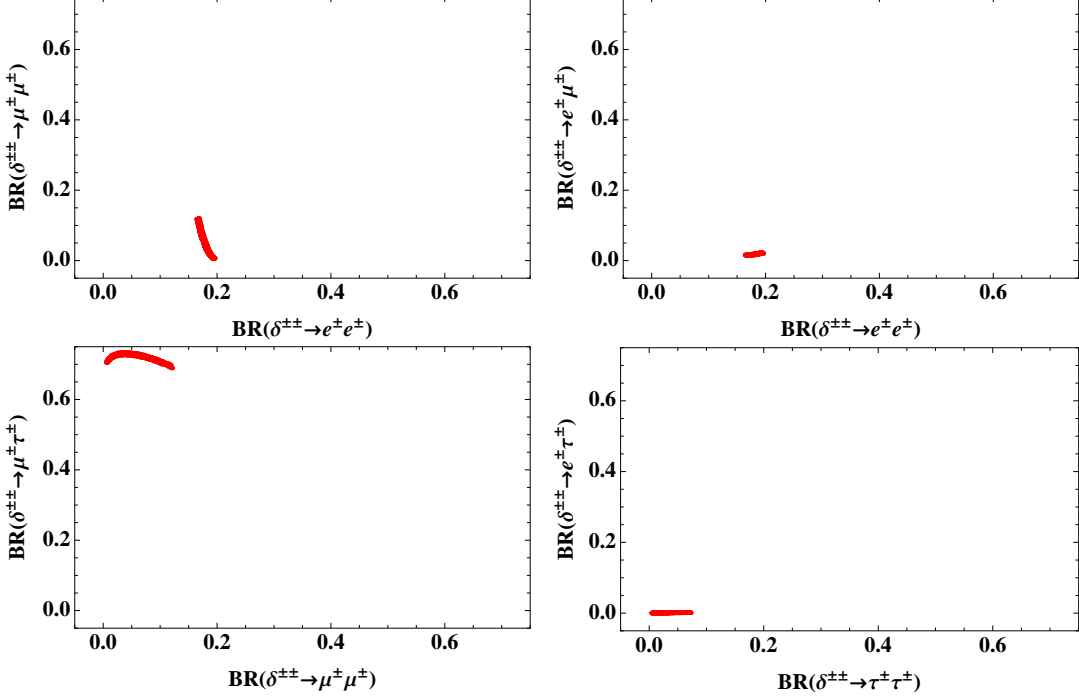


FIG. 10. The same plots as Fig. 6 in the case of Model (4) case B for NO.

where  $\chi \equiv m_e^2 m_\mu^2 + m_\mu^2 m_\tau^2 + m_\tau^2 m_e^2$ . The coefficients  $C_1$ ,  $C_2$  and  $C_3$  are given by  $\hat{Y}_2 \equiv Y e^{u\phi_Y}$ , where  $Y$  is real positive and  $\phi_Y$  is a phase parameter, such that

$$C_1 = (1 + Y^2)^2, \quad (34a)$$

$$C_2 = 64 + 400Y^6 + Y^{12} - 40Y^3(Y^6 - 8) \cos(3\phi_Y) - 16Y^6 \cos(6\phi_Y), \quad (34b)$$

$$C_3 = 16 + 16Y^2 + 36Y^4 + 4Y^6 + Y^8 - 8Y^3(Y^2 - 2) \cos(3\phi_Y). \quad (34c)$$

The values of these coefficients are determined when we fix the value of modulus  $\tau$ . We then obtain the general equations to determine  $\hat{\alpha}$  and  $\hat{\beta}$ :

$$\frac{(1+s)(s+t)}{t} = \frac{(\sum m_i^2/C_1)(\chi/C_3)}{\prod m_i^2/C_2}, \quad \frac{(1+s)}{s+t} = \frac{(\sum m_i^2/C_1)^2}{\chi/C_3}, \quad (35)$$

where  $s \equiv \hat{\alpha}^2 + \hat{\beta}^2$  and  $t \equiv \hat{\alpha}^2 \hat{\beta}^2$ . We thus obtain  $\hat{\alpha}$  and  $\hat{\beta}$  by the relation:

$$\hat{\alpha}_1^2 = \frac{s + \sqrt{s^2 - 4t}}{2}, \quad \hat{\beta}_1^2 = \frac{s - \sqrt{s^2 - 4t}}{2}, \quad (36)$$

$$\hat{\alpha}_2^2 = \frac{s - \sqrt{s^2 - 4t}}{2}, \quad \hat{\beta}_2^2 = \frac{s + \sqrt{s^2 - 4t}}{2}, \quad (37)$$

where we separately write the possible two solutions for  $\hat{\alpha}$  and  $\hat{\beta}$ . Finally  $\tilde{\gamma}$  is determined by  $\hat{\alpha}$  and  $\hat{\beta}$  via Eq. (33a).

For the charged lepton Yukawa couplings with modular weight  $k = 4$ , Eqs. (33) and (34) are given as follows,

$$\text{Tr}[M_E^\dagger M_E] = \sum_{i=e}^{\tau} m_i^2 = \frac{|\tilde{\gamma}Y_3^2|^2}{4}(1 + \hat{\alpha}^2 + \hat{\beta}^2)C_1, \quad (38a)$$

$$\text{Det}[M_E^\dagger M_E] = \prod_{i=e}^{\tau} m_i^2 = \frac{|\tilde{\gamma}Y_3^2|^6}{64}\hat{\alpha}^2\hat{\beta}^2C_2, \quad (38b)$$

$$\frac{\text{Tr}[M_E^\dagger M_E]^2 - \text{Det}[M_E^\dagger M_E]}{2} = \chi = \frac{|\tilde{\gamma}Y_3^2|^4}{16}(\hat{\alpha}^2 + \hat{\alpha}^2\hat{\beta}^2 + \hat{\beta}^2)C_3, \quad (38c)$$

where

$$C_1 = \frac{1}{4}(Y^8 + 4Y^6 + 36Y^4 + 16Y^2 - 8(Y^2 - 2)Y^3 \cos(3\phi_Y) + 16), \quad (39a)$$

$$C_2 = \frac{1}{64}(Y^{12} - 16Y^6 \cos(6\phi_Y) + 400Y^6 - 40(Y^6 - 8)Y^3 \cos(3\phi_Y) + 64)^2, \quad (39b)$$

$$C_3 = \frac{1}{16}(Y^2 + 2)^2(Y^{12} - 16Y^6 \cos(6\phi_Y) + 400Y^6 - 40(Y^6 - 8)Y^3 \cos(3\phi_Y) + 64). \quad (39c)$$

Similarly  $\tilde{\gamma}$  is determined by  $\hat{\alpha}$  and  $\hat{\beta}$  via Eq. (38a).

## ACKNOWLEDGMENTS

This work is supported by MEXT KAKENHI Grant Numbers JP19H04605 (TK), JP18H05543 (T.S.), and JSPS KAKENHI Grant Nos. JP18H01210 (T.S.), JP18K03651 (T.S.).

- 
- [1] R. de Adelhart Toorop, F. Feruglio and C. Hagedorn, Nucl. Phys. B **858**, 437 (2012) [arXiv:1112.1340 [hep-ph]].
- [2] J. Lauer, J. Mas and H. P. Nilles, Phys. Lett. B **226**, 251 (1989). Nucl. Phys. B **351**, 353 (1991).
- [3] W. Lerche, D. Lust and N. P. Warner, Phys. Lett. B **231**, 417 (1989).
- [4] S. Ferrara, D. Lust and S. Theisen, Phys. Lett. B **233**, 147 (1989).
- [5] D. Cremades, L. E. Ibanez and F. Marchesano, JHEP **0405**, 079 (2004) [hep-th/0404229].
- [6] T. Kobayashi and S. Nagamoto, Phys. Rev. D **96**, no. 9, 096011 (2017) [arXiv:1709.09784 [hep-th]].

- [7] T. Kobayashi, S. Nagamoto, S. Takada, S. Tamba and T. H. Tatsuishi, Phys. Rev. D **97**, no. 11, 116002 (2018) [arXiv:1804.06644 [hep-th]].
- [8] T. Kobayashi and S. Tamba, Phys. Rev. D **99** (2019) no.4, 046001 [arXiv:1811.11384 [hep-th]].
- [9] A. Baur, H. P. Nilles, A. Trautner and P. K. S. Vaudrevange, Phys. Lett. B **795**, 7 (2019) [arXiv:1901.03251 [hep-th]]; arXiv:1908.00805 [hep-th].
- [10] Y. Kariyazono, T. Kobayashi, S. Takada, S. Tamba and H. Uchida, Phys. Rev. D **100**, no. 4, 045014 (2019) [arXiv:1904.07546 [hep-th]].
- [11] F. Feruglio, doi:10.1142/9789813238053\_0012 arXiv:1706.08749 [hep-ph].
- [12] J. C. Criado and F. Feruglio, arXiv:1807.01125 [hep-ph].
- [13] T. Kobayashi, N. Omoto, Y. Shimizu, K. Takagi, M. Tanimoto and T. H. Tatsuishi, JHEP **1811**, 196 (2018) [arXiv:1808.03012 [hep-ph]].
- [14] H. Okada and M. Tanimoto, Phys. Lett. B **791**, 54 (2019) [arXiv:1812.09677 [hep-ph]].
- [15] T. Nomura and H. Okada, arXiv:1904.03937 [hep-ph].
- [16] H. Okada and M. Tanimoto, arXiv:1905.13421 [hep-ph].
- [17] F. J. de Anda, S. F. King and E. Perdomo, arXiv:1812.05620 [hep-ph].
- [18] P. P. Novichkov, S. T. Petcov and M. Tanimoto, arXiv:1812.11289 [hep-ph].
- [19] T. Nomura and H. Okada, arXiv:1906.03927 [hep-ph].
- [20] G. J. Ding, S. F. King and X. G. Liu, JHEP **1909**, 074 (2019) [arXiv:1907.11714 [hep-ph]].
- [21] H. Okada and Y. Orikasa, arXiv:1907.13520 [hep-ph].
- [22] T. Nomura, H. Okada and O. Popov, arXiv:1908.07457 [hep-ph].
- [23] T. Kobayashi, Y. Shimizu, K. Takagi, M. Tanimoto and T. H. Tatsuishi, arXiv:1909.05139 [hep-ph].
- [24] T. Asaka, Y. Heo, T. H. Tatsuishi and T. Yoshida, arXiv:1909.06520 [hep-ph].
- [25] D. Zhang, arXiv:1910.07869 [hep-ph].
- [26] T. Kobayashi, K. Tanaka and T. H. Tatsuishi, Phys. Rev. D **98** (2018) no.1, 016004 [arXiv:1803.10391 [hep-ph]].
- [27] T. Kobayashi, Y. Shimizu, K. Takagi, M. Tanimoto, T. H. Tatsuishi and H. Uchida, Phys. Lett. B **794**, 114 (2019) [arXiv:1812.11072 [hep-ph]].
- [28] T. Kobayashi, Y. Shimizu, K. Takagi, M. Tanimoto and T. H. Tatsuishi, arXiv:1906.10341 [hep-ph].
- [29] H. Okada and Y. Orikasa, arXiv:1907.04716 [hep-ph].

- [30] J. T. Penedo and S. T. Petcov, Nucl. Phys. B **939**, 292 (2019) [arXiv:1806.11040 [hep-ph]].
- [31] P. P. Novichkov, J. T. Penedo, S. T. Petcov and A. V. Titov, JHEP **1904**, 005 (2019) [arXiv:1811.04933 [hep-ph]].
- [32] T. Kobayashi, Y. Shimizu, K. Takagi, M. Tanimoto and T. H. Tatsuishi, arXiv:1907.09141 [hep-ph].
- [33] S. F. King and Y. L. Zhou, arXiv:1908.02770 [hep-ph].
- [34] H. Okada and Y. Orikasa, arXiv:1908.08409 [hep-ph].
- [35] J. C. Criado, F. Feruglio, F. Feruglio and S. J. D. King, arXiv:1908.11867 [hep-ph].
- [36] X. Wang and S. Zhou, arXiv:1910.09473 [hep-ph].
- [37] P. P. Novichkov, J. T. Penedo, S. T. Petcov and A. V. Titov, arXiv:1812.02158 [hep-ph].
- [38] G. J. Ding, S. F. King and X. G. Liu, arXiv:1903.12588 [hep-ph].
- [39] I. de Medeiros Varzielas, S. F. King and Y. L. Zhou, arXiv:1906.02208 [hep-ph].  
citeLiu:2019khw
- [40] X. G. Liu and G. J. Ding, arXiv:1907.01488 [hep-ph].
- [41] G. Altarelli and F. Feruglio, Rev. Mod. Phys. **82** (2010) 2701 [arXiv:1002.0211 [hep-ph]].
- [42] H. Ishimori, T. Kobayashi, H. Ohki, Y. Shimizu, H. Okada and M. Tanimoto, Prog. Theor. Phys. Suppl. **183** (2010) 1 [arXiv:1003.3552 [hep-th]].
- [43] H. Ishimori, T. Kobayashi, H. Ohki, H. Okada, Y. Shimizu and M. Tanimoto, Lect. Notes Phys. **858** (2012) 1, Springer.
- [44] D. Hernandez and A. Y. Smirnov, Phys. Rev. D **86** (2012) 053014 [arXiv:1204.0445 [hep-ph]].
- [45] S. F. King and C. Luhn, Rept. Prog. Phys. **76** (2013) 056201 [arXiv:1301.1340 [hep-ph]].
- [46] S. F. King, A. Merle, S. Morisi, Y. Shimizu and M. Tanimoto, arXiv:1402.4271 [hep-ph].
- [47] S. F. King, Prog. Part. Nucl. Phys. **94** (2017) 217 [arXiv:1701.04413 [hep-ph]].
- [48] S. T. Petcov, Eur. Phys. J. C **78** (2018) no.9, 709 [arXiv:1711.10806 [hep-ph]].
- [49] M. C. Chen, S. Ramos-Sánchez and M. Ratz, arXiv:1909.06910 [hep-ph].
- [50] P. P. Novichkov, J. T. Penedo, S. T. Petcov and A. V. Titov, JHEP **1907**, 165 (2019) [arXiv:1905.11970 [hep-ph]].
- [51] T. Kobayashi, Y. Shimizu, K. Takagi, M. Tanimoto, T. H. Tatsuishi and H. Uchida, arXiv:1910.11553 [hep-ph].
- [52] M. Magg and C. Wetterich, Phys. Lett. B **94**, 61 (1980); G. Lazarides, Q. Shafi and C. Wetterich, Nucl. Phys. B **181**, 287 (1981); R. N. Mohapatra and G. Senjanovic, Phys. Rev. D **23**,

- 165 (1981); E. Ma and U. Sarkar, Phys. Rev. Lett. **80**, 5716 (1998) [hep-ph/9802445].
- [53] W. Konetschny and W. Kummer, Phys. Lett. B **70**, 433 (1977); J. Schechter and J. W. F. Valle, Phys. Rev. D **22**, 2227 (1980); T. P. Cheng and L. -F. Li, Phys. Rev. D **22**, 2860 (1980); S. M. Bilenky, J. Hosek and S. T. Petcov, Phys. Lett. B **94**, 495 (1980).
- [54] M. Hirsch, S. Kaneko and W. Porod, Phys. Rev. D **78**, 093004 (2008) [arXiv:0806.3361 [hep-ph]].
- [55] I. Esteban, M. C. Gonzalez-Garcia, A. Hernandez-Cabezudo, M. Maltoni and T. Schwetz, JHEP **1901**, 106 (2019) [arXiv:1811.05487 [hep-ph]].
- [56] N. Aghanim *et al.* [Planck Collaboration], arXiv:1807.06209 [astro-ph.CO].
- [57] CMS Collaboration [CMS Collaboration], CMS-PAS-HIG-16-036.
- [58] M. Aaboud *et al.* [ATLAS Collaboration], Eur. Phys. J. C **78**, no. 3, 199 (2018) [arXiv:1710.09748 [hep-ex]].
- [59] G. Uccielli [ATLAS Collaboration], PoS CHARGED **2018**, 008 (2019).